Tb doping induced enhancement of anomalous Hall effect in NiFe films*

Zhu Jia-Peng(朱嘉鹏)[a], Ma Li(马 丽)[a]†, Zhou Shi-Ming(周仕明)[a], Miao Jun(苗 君)[b], and Jiang Yong(姜 勇)[b]

[a] Shanghai Key Laboratory of Special Artificial Microstructure, Pohl Institute of Solid State Physics, and School of Physics Science and Engineering, Tongji University, Shanghai 200092, China

[b] State Key Laboratory for Advanced Metals and Materials, School of Materials Science and Engineering, University of Science and Technology Beijing, Beijing 100083, China

(Received 30 July 2014; revised manuscript received 7 September 2014; published online 14 November 2014)

$Tb_x(Ni_{0.8}Fe_{0.2})_{1-x}$ films with $x \leq 0.14$ are fabricated and the anomalous Hall effect is studied. The intrinsic anomalous Hall conductivity and the extrinsic one from the impurity and phonon induced scattering both increase with increasing x. The enhancement of the intrinsic anomalous Hall conductivity is ascribed to both the weak spin–orbit coupling enhancement and the Fermi level shift. The enhancement of the extrinsic term comes from the changes of both Fermi level and impurity distribution. In contrast, the in-plane and the out-of-plane uniaxial anisotropies in the TbNiFe films change little with x. The enhancement of the Hall angle by Tb doping is helpful for practical applications of the Hall devices.

Keywords: anomalous Hall effect, magnetic transition alloys, heavy rare earth element, spin–orbit coupling

PACS: 71.70.Ej, 73.50.Jt, 75.47.Np, 75.50.Bb **DOI:** 10.1088/1674-1056/24/1/017101

1. Introduction

Since the anomalous Hall effect (AHE) was discovered in 1880, it has been studied extensively in magnetic alloys both experimentally and theoretically.[1–6] For most magnetic alloys, the anomalous Hall resistivity obeys the conventional scaling law $\rho_{AH} = a\rho_{xx} + b\rho_{xx}^2$, where ρ_{xx} is the longitudinal resistivity. The linear term comes from the skew scattering contribution and the second quadratic term arises from the side-jump and intrinsic contributions. Very recently, a modified scaling law was proposed[7] and the residual resistivity ρ_{xx0} and the phonon induced resistivity ρ_{xxT} were assumed to have different skew parameters, i.e., $\rho_{AH} = a'\rho_{xx0} + a''\rho_{xxT} + b\rho_{xx}^2$. Since ρ_{AH} is often much smaller than ρ_{xx}, the anomalous Hall conductivity (AHC) can be expressed as $\sigma_{AH} \approx -(a'\rho_{xx0} + a''\rho_{xxT})\sigma_{xx}^2 - b$. Karplus and Luttinger pointed out that the intrinsic AHC comes from the interplay between the exchange splitting and the spin–orbit coupling (SOC).[2] It is now interpreted in terms of the Berry phase and expressed as an integral of the Berry curvature over the Bloch states in the $\boldsymbol{k}$ space.[8]

It is essential to address the dependence of the AHE on the physical parameter of magnetic alloys. Although the intrinsic AHC is well known to strongly depend on the SOC strength,[2,6,8] very few experiments have been carried out to study this issue.[9–11] Heavy rare-earth (RE) elements such as Tb and Gd are known to have strong SOC,[12] which manifests itself as a strong perpendicular magnetic anisotropy in TbFeCo and GdFeCo alloy films.[13,14] The SOC effect on the magnetic damping parameter has also been demonstrated.[15–18] Studies of the AHE in heavier RE doped 3d transition alloys might be helpful to deeply understand the effect of the SOC on the AHE. Moreover, many attempts have been made to enhance the Hall angle.[19–21] For example, the Co/Pt multilayers sandwiched by ultrathin MgO layers have been shown to have ultrahigh AHE due to the surface modification.[19] Ultrahigh sensitive AHE has also been observed in SiO_2/FePt/SiO_2 sandwiches due to the interface scattering.[20] In Tb-doped NiFe alloys, the magnetic damping parameter is found to be enhanced, in comparison with NiFe alloys, suggesting the enhancement of the magnetic anisotropy. Accordingly, the Hall angle in the TbNiFe alloys is expected to be enhanced compared with that of the NiFe alloys. In this work, the Hall angle is enhanced in $Tb_x(Ni_{0.8}Fe_{0.2})_{1-x}$ by Tb doping in NiFe films. It is found that the ρ_{xx} independent term b, and the a' and a'' increase with increasing x. The enhancement of b is caused by the changes of the intrinsic AHC and the side-jump terms in the Kubo formalism.[22] In particular, the a'' and a' enhancement is possibly due to the interplay among the elastic scattering, the inelastic scattering, and the SOC. In contrast, the in-plane and the out-of-plane magnetic anisotropic constants are found to change little with x.

*Project supported by the National Natural Science Foundation of China (Grant Nos. 11374227, 51331004, 51171129, and 51201114), the Shanghai Science and Technology Committee, China (Grant Nos. 0252nm004, 13XD1403700, and 13520722700), and the National Basic Research Program of China (Grant No. 2015CB921501).

†Corresponding author. E-mail: 77shibihan@tongji.edu.cn

© 2015 Chinese Physical Society and IOP Publishing Ltd

2. Experiments

A series of 20 nm thick $Tb_x(Ni_{0.8}Fe_{0.2})_{1-x}$ (TbNiFe) films were fabricated on glass substrates at ambient temperature by DC magnetron sputtering. Small pieces of Tb were put on the $Ni_{0.8}Fe_{0.2}$ alloy target to form the TbNiFe target. The Tb concentration was controlled by changing the numbers of Tb pieces. The base pressure of the fabrication system was 1.0×10^{-5} Pa and the Ar pressure was 0.35 Pa during deposition. The deposition rate of the TbNiFe film was about 1.0 nm/s. The film thickness was controlled by the deposition time and was finally determined by the X-ray diffraction reflectivity (XRR) at small angles. The microstructure was measured by X-ray diffraction (XRD). The alloy composition was determined by energy dispersive X-ray (EDX) spectroscopy in combination with scanning electronic microscopy (SEM). Hysteresis loops were measured by a vibrating sample magnetometer (Lake Shore 7407-VSM) at room temperature. The angular dependent ferromagnetic resonance (FMR) spectra at 9.78 GHz were measured at room temperature with the external magnetic field H parallel and perpendicular to the film plane. The ρ_{xx} and ρ_{AH} at various temperatures were measured with a standard Hall bar by a physics properties measurement system (Quantum Design PPMS-9T system).

3. Results and discussion

From the oscillation period in the XRR fringe patterns in Fig. 1(a), the film thickness and the root mean square (RMS) surface roughness are estimated. For example, the film thickness is fitted to be 20 ± 1 nm, close to the designed value. From the XRR spectra, the RMS surface roughness is 0.87 nm, 1.19 nm, and 1.02 nm for $x = 0$, 0.10, and 0.14, respectively. The RMS surface roughness slightly increases after the NiFe films are doped with Tb. In addition to the strong broad peak near $2\theta = 23°$ from the amorphous glass substrate, there is a broad and weak diffraction peak near $2\theta = 44°$, indicating the preferred orientation of FCC (111) of permalloy, as shown in Fig. 1(b). The intensity and the width of the diffraction peak change little with x, as shown for $x = 0$ and 0.14 samples.

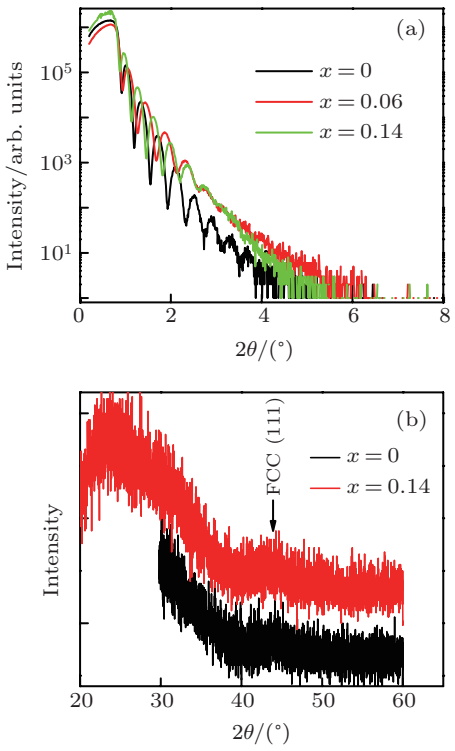


Fig. 1. (color online) (a) XRR at small angles and (b) XRD at high angles for TbNiFe films. In panel (b), the curves are shifted for clarification.

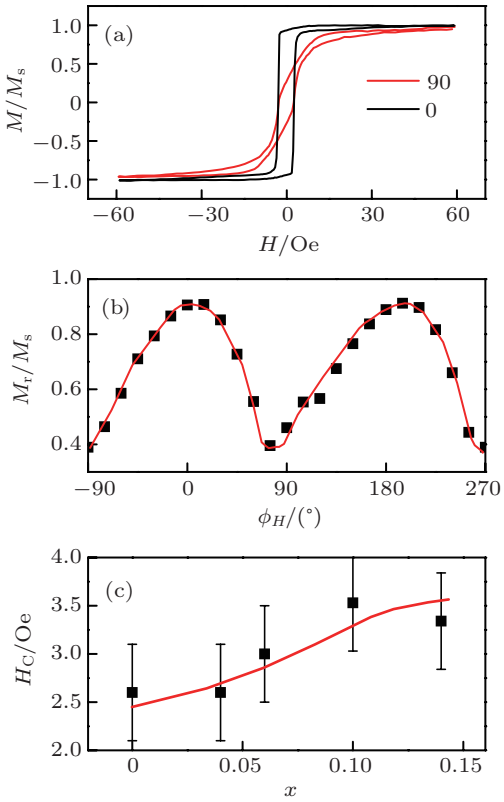


Fig. 2. (color online) (a) Typical in-plane hysteresis loops along the easy axis and the hard axis, and the numbers refer to the values of ϕ_H. (b) The angular dependence of the remanent ratio, where ϕ_H refers to the angle between H and the easy axis. (c) The x dependence of the coercivity. The red lines in panels (b) and (c) serve as a guide to the eye.

Figure 2(a) shows the in-plane angular dependent hysteresis loops of a typical sample ($x = 0.14$). One can find that the in-plane coercivity almost does not change with the orientation of H, whereas the remanent ratio changes significantly. It is equal to 1.0 along the easy axis and is reduced when H deviates from the easy axis, as shown in Fig. 2(b). The two-fold symmetry of the angular dependent remanent ratio clearly shows the in-plane uniaxial magnetic anisotropy for small samples. The coercivity almost keeps constant for all x and slightly increases for large x, as shown in Fig. 2(c). Meanwhile, the spontaneous magnetization M_S at room temperature equals 720 emu/cm^3, 583 emu/cm^3, 543 emu/cm^3, 515 emu/cm^3, and 484 emu/cm^3 for $x = 0$, 0.04,

0.06, 0.10, and 0.14, respectively. In order to study the magnetic anisotropy, FMR measurements were performed at room temperature. Figures 3(a) and 3(b) show the in-plane and the out-of-plane angular dependent resonance fields of the typical samples. To calculate the in-plane and the out-of-plane magnetic anisotropies, the approach of Suhl and Gerhardter *et al.* is used.[23,24] It is found that the in-plane and the out-of-plane uniaxial magnetic anisotropic constants $K_{\mathrm{U-IP}}$ and $K_{\mathrm{U-OOP}}$ are randomly scattered as a function of x because the former and the latter ones are about one and three orders of magnitude smaller than the demagnetization energy, respectively, which agrees with the results in Fig. 2(c). For TbNiFe alloy films with $x \leq 0.14$, no prominent SOC effects on the magnetic anisotropic constants are observed, which agrees with the observation in TbFeCo and GdFeCo alloys that a strong perpendicular magnetic anisotropy occurs only in a narrow composition window (20 at.% to 25 at.%) of Tb and Gd atomic concentrations.[13,14]

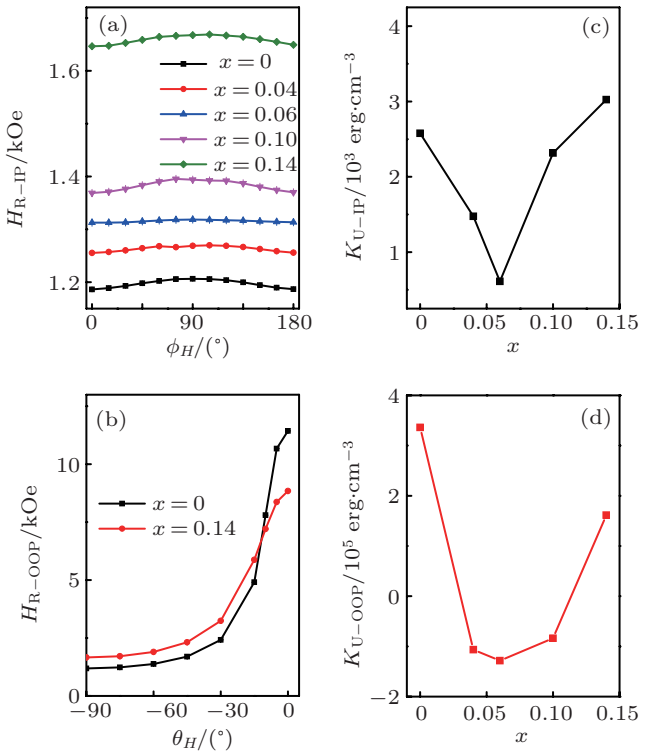


Fig. 3. (color online) Angular dependences of in-plane and out-of-plane resonance fields (a) $H_{\mathrm{R-IP}}$ and (b) $H_{\mathrm{R-OOP}}$, and in-plane and out-of-plane anisotropy constants (c) $K_{\mathrm{U-IP}}$ and (d) $K_{\mathrm{U-OOP}}$ as a function of x. Solid lines in panels (a) and (b) serve as a guide to the eye. Here ϕ_H (θ_H) refers to the angle between H and the in-plane easy axis (the film normal direction).

Figures 4(a) and 4(b) show the temperature (T) dependences of ρ_{xx} and ρ_{AH} for different x, respectively. For all samples, ρ_{xx} decreases with decreasing T and approaches the residual resistivity ρ_{xx0} at low T due to the impurity scattering, obeying the Matthiessen's rule. At high T, ρ_{xx} approximately changes in a linear fashion. The ρ_{xx0} increases significantly with increasing x. It is about 40 Ω·cm and 200 Ω·cm for $x = 0$ and 0.14, respectively. This may be due to the degraded microstructure for large x. As is well known, the TbFeCo films are of either an amorphous structure or nanocrystalline at high Tb contents.[13,14] In experiments, the Hall loops at various T were measured under H perpendicular to the film plane. The Hall resistivity ρ_{xy} generally consists of two components contributed by an ordinary Hall effect and AHE. For the out-of-plane H larger than the saturation magnetic field, ρ_{xy} changes as a linear function of H due to the Lorentz force. For small H, ρ_{AH} is assumed to be proportional to the magnetization of the magnetic alloys. Accordingly, ρ_{AH} is extrapolated from ρ_{xy} at high H. For large x, ρ_{AH} is found to decrease with increasing T, whereas it almost does not change for small x, as shown in Fig. 4(b). The ρ_{AH} is about two orders of magnitude smaller than ρ_{xx}. At a specific T, ρ_{AH} increases monotonically with increasing x. In experiments, the AHE in the TbNiFe alloys does not obey the conventional scaling law. It is noted that the spontaneous magnetization of all samples almost does not change with T and the effect of the varying magnetization is negligible,[10] as shown in the inset of Fig. 4(d). Here, we adopt the modified approach proposed by Tian *et al.*[7] For all samples, the ρ_{AH} versus ρ_{xx} curve can be fitted by the new approach, as shown in Figs. 4(c) and 4(d), and a' and b are both positive whereas a'' is negative. Take $x = 0.14$ for example, one has $a' = 100$, $a'' = -0.9$, and $b = 1.8$ mS/cm. Moreover, for large x, the magnitude of a'' is much smaller than that of

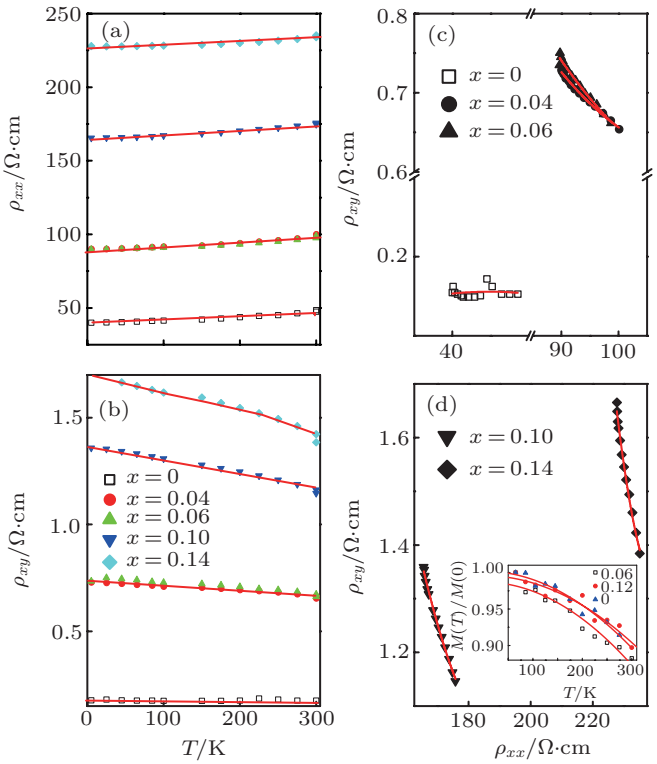


Fig. 4. (color online) The T dependences of (a) ρ_{xx} and (b) ρ_{AH} for TbNiFe films, and ρ_{AH} versus ρ_{xx} for (c) $x = 0$, 0.04, 0.06 and (d) $x = 0.10$, 0.14. The red lines serve as a guide to the eye in panels (a) and (b) and are fitted results in panels (c) and (d) using the modified scaling law. Normalized M versus T curves for selected samples are also shown in the inset.

a', indicating the smaller contribution of ρ_{xxT} than that of ρ_{xx0}, whereas they are comparable for $x = 0$.[25] Similar phenomena are also observed for epitaxially grown Fe films.[7] Figures 5(a)–5(c) show a', a'', and b each as a function of x. The three parameters change little for small x and then increase for large x.

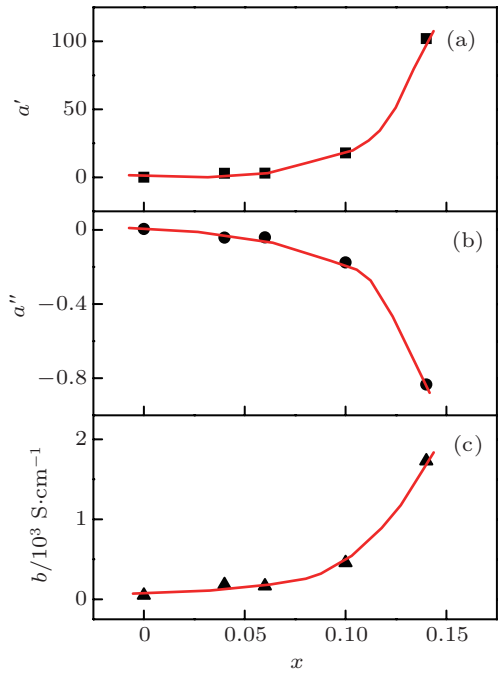


Fig. 5. (color online) Dependences of (a) a', (b) a'', and (c) b on x. Solid lines serve as a guide to the eye.

It is essential to reveal the connection between the AHE behavior and the microstructural and magnetic properties. When the Tb content increases, the effective SOC should be enhanced slightly with the Tb doping. Although the ρ_{xx} independent term b is argued to equal the intrinsic AHC within the new fitting approach,[7] the b should consist of the intrinsic AHC and the side-jump one, and the latter one is suppressed by the inelastic scattering at $T > 0$.[26] The intrinsic AHC can be tuned by the SOC strength, as observed in ordered and disordered FePdPt alloys.[8,10,11] According to the theoretical model,[22] the side-jump term strongly depends on the Fermi level.[22] The effect of the varying SOC strength and Fermi level on the intrinsic AHC and the side-jump term in the TbNiFe films should be considered when the effective SOC strength and the Fermi level may both change with x. The TbNiFe films tend to become amorphous and have large surface roughness, as demonstrated by the enhancement of ρ_{xx0} in Fig. 4(a). Since the skew parameter increases with the increasing impurity scattering, a' is enhanced.[26] Similar phenomena have been observed in other systems. For epitaxial Fe films, a' and ρ_{xx0} are both found to be enhanced for thin films, which is ascribed to the enhanced scattering from the film surface. For L1(0) FePdPt films, the skew parameter and ρ_{xx0} both acquire maximal values when the Pd and Pt atomic concentrations are close to each other.

It is interesting to find that a'' also increases in magnitude with increasing x, although it is much smaller than a'. The extrinsic contribution of the phonon scattering was studied theoretically very recently.[26] With increasing x, the films favor becoming amorphous. Due to the high order perturbation of the randomly distributed potential in disordered alloys, the increase of the impurity scattering may indirectly lead to increasing a''. Secondly, arising from the asymmetric scattering due to the SOC, the skew scattering contribution increases with increasing SOC strength for weak SOC.[27] The a'' enhancement is therefore caused by the interplay among the elastic scattering from the impurity sites, the inelastic scattering from the excited phonon at $T > 0$, and the SOC. Finally, the Hall angle is also enhanced with Tb doping, and acquires a maximal value at $x = 0.06$. At room temperature, it is equal to 3.6×10^{-3}, 6.7×10^{-3}, 6.50×10^{-3}, and 5.88×10^{-3} for $x = 0$, 0.06, 0.10, and 0.14, respectively. The Hall angle in the TbNiFe films is close to that in MgO/Co/Pt/MgO sandwiches.[19] As analyzed above, the enhancement of the Hall angle is mainly attributed to the larger a' and b with Tb doping.

4. Summary

The TbNiFe films with various Tb contents were fabricated, and the magnetic and magnetotransport properties were studied as a function of the Tb content x. The following results are obtained. The in-plane coercivity, in-plane and out-of-plane uniaxial anisotropic constants are not influenced by Tb doping. In contrast, the Hall angle is enhanced significantly with Tb doping. The ρ_{xx} independent AHC and the skew parameter are both found to increase by the Tb doping. The increase of the intrinsic term may come from both the enhancement of the effective SOC and the shift of the Fermi level. The enhancement of the extrinsic AHC may stem from the Fermi level shift and the microstructure degradation. The heavier RE doping in 3d transition alloys will provide a new approach to enhance the AHE, which is helpful for practical applications of high sensitivity Hall devices.

References

[1] Hall E H 1881 *Mag. Philos.* **12** 157
[2] Karplus R and Luttinger J M 1954 *Phys. Rev.* **95** 1154
[3] Smit J 1958 *Physica* (Amsterdam) **21** 877
[4] Smit J 1958 *Physica* **24** 39
[5] Berger L 1970 *Phys. Rev. B* **2** 4559
[6] Nagaosa N, Sinova J, Onoda S, MacDonald A H and Ong N P 2010 *Rev. Mod. Phys.* **82** 1539
[7] Tian Y, Ye L and Jin X F 2009 *Phys. Rev. Lett.* **103** 087206
[8] Yao Y G, Kleinman L, MacDonald A H, Sinova J, Jungwirth T, Wang D, Wang E and Niu Q 2004 *Phys. Rev. Lett.* **92** 037204

[9] Seemann K M, Mokrousov Y, Aziz A, Miguel J, Kronast F, Kuch W, Blamire M G, Hindmarch A T, Hickey B J, Souza I and Marrows C H 2010 *Phys. Rev. Lett.* **104** 076402
[10] He P, Ma L, Shi Z, Guo G Y, Zheng J G, Xin Y and Zhou S M 2012 *Phys. Rev. Lett.* **109** 066402
[11] Ma L, He P, Gao W B, Zhou S M, Shi Z, Miao J and Jiang Y 2013 *J. Appl. Phys.* **114** 243912
[12] Jensen J and Mackintosh A R 1991 *Rare Earth Magnetism: Structures and Excitations* (Oxford: Clarendon Press)
[13] Takayama S, Niihara T, Kaneko K, Sugita Y and Ojima M 1987 *J. Appl. Phys.* **61** 2610
[14] Carey R, Newman D M and Thomas B W J 1995 *J. Phys. D: Appl. Phys.* **28** 2207
[15] Radu I, Woltersdorf G, Kiessling M, Melnikov A, Bovensiepen U, Thiele J U and Back C H 2009 *Phys. Rev. Lett.* **102** 117201
[16] Rebei A and Hohlfeld J 2006 *Phys. Rev. Lett.* **97** 117601
[17] Reidy S G, Cheng L and Bailey W E 2003 *Appl. Phys. Lett.* **82** 1254
[18] Zhang W, Jiang S, Wong P K J, Sun L, Wang Y K, Wang K, de Jong M P, van der Wiel W G, van der Laan G and Zhai Y 2014 *J. Appl. Phys.* **115** 17A308
[19] Zhang S L, Teng J, Zhang J Y, Liu Y, Li J W, Yu G H and Wang S G 2010 *Appl. Phys. Lett.* **97** 222504
[20] Lu Y M, Cai J W, Pan H Y and Sun L 2012 *Appl. Phys. Lett.* **100** 022404
[21] Zhang S L, Liu Y, Collins-McIntyre L J, Hesjedal T, Zhang J Y, Wang S G and Yu G H 2013 *Sci. Rep.* **3** 2087
[22] Sinitsyn N A, MacDonald A H, Jungwirth T, Dugaev V K and Sinova J 2007 *Phys. Rev. B* **75** 045315
[23] Suhl H 1955 *Phys. Rev.* **97** 555
[24] Gerhardter F, Li Y and Baberschke K 1993 *Phys. Rev. B* **47** 11204
[25] Zhang Y Q, Sun N Y, Shan R, Zhang J W, Zhou S M, Shi Z and Guo G Y 2013 *J. Appl. Phys.* **114** 163714
[26] Shitade A and Nagaosa N 2012 *J. Phys. Soc. Jpn.* **81** 083704
[27] Wölfle P and Muttalib K A 2006 *Ann. Phys.* **15** 508